J|A|C|S
COMMUNICATIONS

Published on Web 09/08/2006

TEM-Induced Structural Evolution in Amorphous Fe Oxide Nanoparticles

Andrew H. Latham,[†,§] Mark J. Wilson,[‡,§] Peter Schiffer,[‡,§] and Mary Elizabeth Williams*[,†,§]

Departments of Chemistry and Physics and Materials Research Institute, The Pennsylvania State University, University Park, Pennsylvania 16802

Received June 30, 2006; E-mail: mbw@chem.psu.edu

Remarkable innovations in nanomaterials synthesis have led to heterocomposites with tunable chemical reactivity and physical properties. A widespread approach has been to use concentric layers coated on the outside of spherical particles to produce core−shell structures.[1] For example, it is now common to encapsulate CdSe nanocrystals in a shell of ZnS to improve the photophysical properties.[1a] Au has been reduced onto the surface of Ag nanoparticles[1b] and onto the surface of Fe_2O_3.[1c] Coated magnetic particles are becoming increasingly important in emerging nanobiotechnologies,[2] and evaluation and confirmation of their structures are central concerns. One of the foremost tools for assessing nanoscale heterostructures is transmission electron microscopy (TEM), since differences in electron density are evidenced as changes in contrast in the images. While it has been known for some time that fluctuations in Au crystal structure upon exposure to an electron beam can occur,[3] and that high energy irradiation can cause Au nanoparticle coalescence,[4] there are no analogous studies using magnetic or core−shell nanoparticles. In this communication, we report for the first time spherical shells of Fe oxide and Fe that evolve from amorphous solid particles during exposure to the beam of the TEM and bear striking resemblance to core−shell structures.[5]

While attempting to prepare monodisperse core−shell γ-Fe_2O_3 nanoparticles, we turned to the method employed for the preparation of core−shell CdSe−ZnS semiconductor nanocrystals.[6] With the use of this approach, particles are first nucleated and grown from $Fe(CO)_5$ in a mixture of trioctylphosphine oxide (TOPO) and hexadecylamine (HDA), which serve as both stabilizing ligand and solvent and are present in a ∼25:1 ligand to Fe molar ratio (see Supporting Information, SI, for details). For comparison, we also employed a well-known procedure for synthesizing γ-Fe_2O_3 nanoparticles that uses the thermal decomposition of $Fe(CO)_5$ in the presence of an acid-terminated surfactant (i.e., lauric acid) in a high boiling solvent (i.e., octyl ether).[7] Following growth, the particles from both preparations are oxidized in air at 80 °C for a minimum of 14 h to produce the Fe oxides.

The particles were first examined in a low resolution TEM: Figure 1 compares images of the Fe oxide particles prepared using lauric acid and HDA/TOPO. In both cases, the particles are spherical and relatively uniform in size. The average diameter of lauric acid stabilized particles is 8.5 ± 0.5 nm, and the HDA/TOPO particles' diameter is 11.8 ± 1.4 nm. The remarkable difference between the two samples is the hollow appearance of the latter. Using variable tilt angles, we confirmed that the particles shown in Figure 1B are spheres and not rings on the grid surface (SI).

The formation of hollow, amorphous Fe oxide shells under the HDA/TOPO conditions is unexpected because no template is present. To understand the differences in morphology that arise

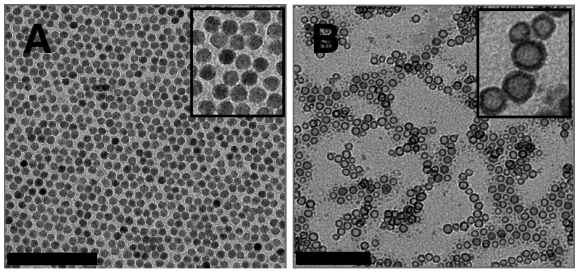

Figure 1. TEM images of Fe oxide nanoparticles synthesized with (A) lauric acid in octyl ether and (B) HDA/TOPO; exposure times, (A) 15 min and (B) 5 min. Scale bars = 100 nm.

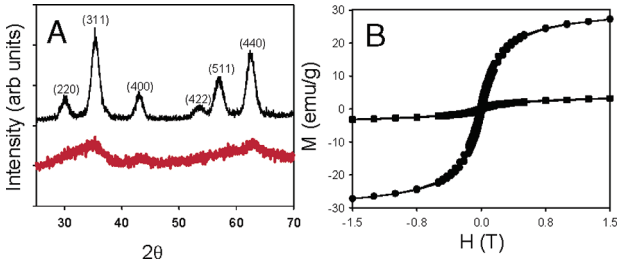

Figure 2. Characterization of the as-prepared particles: (A) XRD patterns of HDA/TOPO (red line) and lauric acid (black line) Fe oxide nanoparticles; and (B) normalized magnetization measurements at 10 K for (■) HDA/TOPO and (●) lauric acid Fe oxide particles.

from the two preparations, we obtained powder diffraction (XRD) and SQUID magnetometry data for both sets of as-prepared particles. In Figure 2A, the XRD of the lauric acid stabilized particles is consistent with crystalline γ-Fe_2O_3, whereas the HDA/TOPO particles are amorphous Fe oxide. SQUID analysis further confirms a substantial difference between the two samples. In Figure 2B, the γ-Fe_2O_3 nanoparticles have a saturation magnetization approaching ∼30 emu/g, whereas the as-prepared amorphous Fe oxide particles have a 10-fold lower magnetization of ∼3 emu/g. Both samples are superparamagnetic with blocking temperatures of 42 and 14 K, respectively (SI). The lower saturation magnetization and blocking temperature is a result of the lack of crystallinity in the HDA/TOPO Fe oxide particles. However, BET analysis of both sets of the as-prepared particle samples revealed that neither is porous; the room temperature EPR spectra of the two samples are similarly identical (see SI).

We therefore turned to detailed high resolution electron microscopy studies to more extensively investigate these nanoscale structures. Using a prealigned 80 keV (∼200 pA/cm^2) electron beam, it was possible to capture images of the particles as a function of time. Surprisingly, we observed that the amorphous Fe oxide particles appeared to be solid spheres at short times, and that they appeared to *evolve into larger, hollow spheres* while exposed to the electron beam. Figure 3 contains sequential TEM images of the same area of the grid taken over the course of 120 s. By moving

† Department of Chemistry.
‡ Department of Physics.
§ Materials Research Institute.

10.1021/ja064666q CCC: $33.50

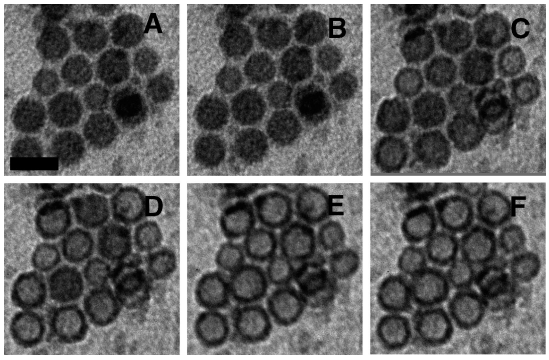

Figure 3. Low resolution TEM images of amorphous Fe oxide particles acquired at approximately (A) 0; (B) 20; (C) 40; (D) 50; (E) 60; and (F) 120 s exposure in the 80 keV beam. Scale bar is 15.

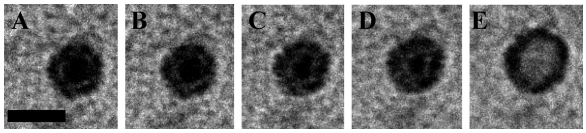

Figure 4. TEM images of a HDA/TOPO-stabilized Fe nanoparticle after (A) 0; (B) 20; (C) 40; (D) 60; and (E) 120 s exposure to the electron beam. Scale bar is 15 nm.

the location of the grid, structural evolution of particles that had not already been exposed to the electron beam was again observed. The change in geometry is directly attributed to irradiation; formation of hollow spheres is irreversible and no additional rearrangements are observed. Analysis of the particle sizes in Figure 3 reveals that these are initially 10.5 ± 1.4 nm in diameter, and over the course of re-structuring, the particles become larger. The average inner and outer diameters of the resultant spheres in Figure 3F are 6.7 ± 1.3 and 11.8 ± 1.4 nm, respectively. This effect was observed for several separate particle preparations in which the initial size was varied between 8 and 18 nm. In comparison, no structural changes are observed in crystalline γ-Fe_2O_3 nanoparticles, even after 15 min of intense irradiation (see SI).

In attempts to repeat the experiment in a high resolution TEM, only hollow spheres were observed, however the particles are exposed to high energy (200 keV) before it is possible to acquire images (~2 min). High resolution images of the particles contain lattice fringes and result in well defined diffraction patterns that are indicative of crystallinity in the shell structures. High resolution EELS mapping, which provided spatially defined elemental analysis of a single particle, conclusively showed that the particles are hollow and the shell contains both Fe and O (see SI).

To test whether this effect was a result of oxidation state, we also examined HDA/TOPO Fe particles that had not been aerated and fully oxidized. Although these are synthesized under air-free conditions, a small amount of surface oxidation occurs during transfer into the TEM because of the reactivity of the Fe metal surface.[8] TEM images taken at short times, such as in Figure 4A, therefore reveal a thin shell of lighter contrast material attributed to the oxide shell. Figure 4 shows that upon electron beam exposure for 2 min, the initially solid particles again evolve into hollow spheres that are strikingly similar in appearance to other reports of core−shell Fe oxide particles.[5] In our experiments, we conclude that hollow particle formation is not a function of Fe oxidation state, and it is therefore unlikely that the mechanism is electron beam induced reduction.

We attribute the changes in particle appearance in Figures 3 and 4 to structural rearrangement as a result of electron beam exposure. The fact that this is observed only for amorphous particles suggests that crystal defects or voids within the Fe oxide are necessary. Although nanoparticle melting points are known to decrease with size,[9] we rule out particle melting as the operative mechanism because neither liquidation nor coalescence of the particles is observed. We similarly rule out phase changes that are known to occur in Fe oxides at high temperatures.[10] Instead, the evolution in morphology is attributed to quasi-melting,[11] in which particle restructuring is the result of fluidlike behavior of atoms or clusters of atoms to reach a thermodynamically favored configuration. For example, coalescence of voids (which may contain solvent or ligand molecules) into a sphere (the hollow core of the particles) would minimize their surface area. It is believed that the energy barriers between conformations in nanoparticles are relatively small and can be easily overcome with a small amount of energy.[10] A quasi-molten state in crystalline Au particles has been observed at higher electron beam fluxes and higher temperatures.[10]

Coalescence of voids *during* synthesis of CoO and Co_xS_y[12] and Fe_xO_y[7] particles has been reported; our results conclusively show hollow particles forming when induced by the TEM *postsynthesis*. Since TEM imaging is the primary tool used for confirmation of core−shell structure, our observation that amorphous Fe oxide and Fe particles exhibit significant reorganization during irradiation by a high energy electron beam implies that caution is necessary during the analysis of core−shell and heterostructured nanoparticles. Given the dearth of alternative analytical methods, time-resolved TEM imaging may be necessary to rule out in situ rearrangements that would preclude accurate assessment of as-prepared particle morphology.

Acknowledgment. We gratefully acknowledge the assistance with acquiring the high resolution data by Joseph Kulik at the Penn State Materials Research Institute TEM facility and the helpful suggestions of Professor Elizabeth Dickey. This work was supported by an NSF CAREER award (Grant CHE0239-702), a Sloan Fellowship, and an Untenured Faculty Grant from 3M. P.S. acknowledges support from NSF Grants DMR-0401486 and DMR-0213623.

Supporting Information Available: Full experimental details and HRTEM, EELS, as well as complete particle characterization. This material is available free of charge via the Internet at http://pubs.acs.org.

References

(1) (a) Dabbousi, B. O.; Rodriguez-Viejo, J.; Mikulec, F. V.; Heine, J. R.; Mattoussi, H.; Ober, R.; Jensen, K. F.; Bawendi, M. G. *J. Phys. Chem. B* **1997**, *101*, 9463−9475. (b) Cao, Y.; Jin, R.; Mirkin, C. A. *J. Am. Chem. Soc.* **2001**, *123*, 7961−7962. (c) Lyon, J. L.; Fleming, D. A.; Stone, M. B.; Schiffer, P.; Williams, M. E. *Nano Lett.* **2004**, *4*, 719−723. (d) Cushing, B. L.; Kolesnichenko, V. L.; O'Connor, C. J. *Chem. Rev.* **2004**, *104*, 3893−3946. (e) Vasquez, Y.; Sra, A. K.; Schaak, R. E. *J. Am. Chem. Soc.* **2005**, *127*, 12504−12505.

(2) *Nanobiotechnology: Concepts, Applications and Perspectives*; Niemeyer, C. M., Mirkin, C. A., Eds.; Wiley-VCH: Weinheim, Germany, 2004.

(3) (a) Bovin, J. O.; Wallenber, R.; Smith, D. *Nature* **1985**, *317*, 47−49. (b) Iijima, S.; Ichihashi, T. *Phys. Rev. Lett.* **1986**, *56*, 616−619.

(4) José-Yacamán, M.; Gutierrez-Wing, C.; Miki, M.; Yang, D.-Q.; Piyakis, K. N.; Sacher, E. *J. Phys. Chem. B* **2005**, *109*, 9703−9711.

(5) Peng, S.; Wang, C.; Xie, J.; Sun, S. *J. Am. Chem. Soc.* **2006**, *128*, 10676−10677.

(6) Talapin, D. V.; Rogach, A. L.; Kornowski, A.; Haase, M.; Weller, H. *Nano Lett.* **2001**, *1*, 207−211.

(7) Hyeon, T.; Lee, S. S.; Park, J.; Chung, Y.; Na, H. B. *J. Am. Chem. Soc.* **2001**, *123*, 12798−12801.

(8) Wang, C. M.; Baer, D. R.; Thomas, L. E.; Amonette, J. E.; Antony, J.; Qiang, Y.; Duscher, G. *J. Appl. Phys.* **2005**, *98*, 094308.

(9) Ding, F.; Rosén, A.; Bolton, K. *Phys. Rev. B* **2004**, *70*, 075416.

(10) Sun, S.; Zeng, H.; Robinson, D. B.; Raoux, S.; Rice, P. M.; Wang, S. X.; Li, G. *J. Am. Chem. Soc.* **2004**, *126*, 273−279.

(11) Marks, L. D. *Rep. Prog. Phys.* **1994**, *57*, 603−649.

(12) Yin, Y.; Rioux, R. M.; Erdonmez, C. K.; Hughes, S.; Somorjai, G. A.; Alivisatos, A. P. *Science* **2004**, *304*, 711−714.

JA064666Q